Materials Letters 220 (2018) 222–225

Contents lists available at ScienceDirect

Materials Letters

journal homepage: www.elsevier.com/locate/mlblue

Featured Letter

# Effect of outdoor temperature on the power-conversion efficiency of newly synthesized organic photosensitizer based dye-sensitized solar cells

Umer Mehmood [a,b], M. Irfan Malik [c], Anwar Ul Haq Khan [a], Ibnelwaleed A. Hussein [d,*], Khalil Harrabi [e], Amir Al-Ahmed [b]

[a] Department of Polymer and Process Engineering, University of Engineering & Technology Lahore, Pakistan
[b] Center of Research Excellence in Renewable Energy, King Fahd University of Petroleum & Minerals (KFUPM), Dhahran, Saudi Arabia
[c] Chemical Engineering Department, KFUPM, Dhahran, Saudi Arabia
[d] Gas Processing Center, Qatar University, Doha, Qatar
[e] Department of Physics, KFUPM, P.O. Box 5050, Dhahran 31261, Saudi Arabia

ARTICLE INFO

*Article history:*
Received 2 February 2018
Received in revised form 3 March 2018
Accepted 8 March 2018
Available online 9 March 2018

*Keywords:*
Outdoor temperature
Organic photosensitizer
Photovoltaics
Dye-sensitized solar cell
Open circuit voltage
Efficiency

ABSTRACT

In this work, organic photosensitizer has been synthesized for dye-sensitized solar cells (DSSCs). The solar cells then fabricated have been characterized by photocurrent-voltage characteristics and electrochemical impedance spectroscopic (EIS) measurements. The effect of outdoor temperature on the photovoltaic performance of DSSCs has also been investigated here. The results indicate that DSSC shows power conversion efficiency of 2.58% at 25 °C under air mass (AM) 1.5 G illumination at 100 mW/cm$^2$. It has also been found out that the efficiency of DSSCs drops with the rise of temperature. The decrease in efficiency can be attributed to decrease in open-circuit voltage of cells. The EIS analysis shows that increase in temperature also reduces the charge recombination resistance mainly due to decrease of electron lifetime. These findings demonstrate that the cell is stable up to 35 °C.



## 1. Introduction

Dye-sensitized solar cells because of their low cost and easy fabrication process have received considerable global attention [1–3]. Dye is the heart of any DSSC, normally it is adsorbed on a semiconducting material ($TiO_2$ is the most commonly used semiconducting material). Upon absorbing the sunlight, it produces excitons [4–6] and transfers electrons to the conduction band of semiconductor. Presently, ruthenium complexes based DSSCs possess the best power conversion efficiencies (PCEs) under standard illumination of AM 1.5 G [5,7,8]. However, the high cost and scarcity of ruthenium are major drawbacks in the metal complex sensitizers [9]. To overcome these problems, metal free organic sensitizers have been synthesized [10]. The basic structural unit of organic dye is donor-π-acceptor. The π-conjugated spacer splits the donor and the acceptor moieties. To form efficient photosensitizers, it has been suggested that the donor groups should be chosen from the electron rich aryl amines family like phenylamine, aminocoumarin, indoline, (difluorenyl)triphenylamine and biphenyl [10]. However, compounds containing thiophene and oxadiazol units due to their outstanding charge transfer characteristics could be efficient π-conjugated spacers. Acrylic acid group as an acceptor moiety is considered as the best option for organic photosensitizers [11]. So far, organic dye based DSSCs have achieved 10.2% PCE [12].

Instead of high cost, another important challenge for the commercialization of DSSCs is the low stability. DSSCs have to fulfill the stability criteria in order to penetrate the photovoltaic market. Temperature is considered as the most crucial outdoor parameter that affects the stability of DSSCs [13]. Liquid electrolytes due to their outstanding electric conductivity show high power conversion efficiency. However, they limit the outdoor applications due to their low boiling points and evaporation over time. To penetrate into the photovoltaic market, liquid electrolyte based DSSCs have to pass stability tests (resistance against humidity and temperature) [14]. Very few papers have highlighted the effect of temperature on the stability of DSSCs during the past decade [15,16]. M. Grätzel designed a DSSC capable of bearing an aging at 80 °C for 1000 h. Moreover, a device also showed stable photovoltaic

* Corresponding author.
*E-mail address:* ihussein@qu.edu.qa (I.A. Hussein).

https://doi.org/10.1016/j.matlet.2018.03.055
0167-577X/

performance up to at 60 °C under AM 1.5 illumination of visible light [17]. Dai et al constructed a 500 W power station with DSSCs modules and investigated the stability under outdoor condition. They observed the degradation in the photovoltaic performance of DSSCs modules under full sunlight illumination [18,19].

Thus it can be concluded that the stability and cost are two major challenges for the commercialization of DSSCs. The aim of this study is to synthesize a low cost organic dye for DSSCs and to examine the influence of temperature on the stability of DSSCs. Though in this case the power conversion efficiency (PCE) is not high but results indicate that the performance of DSSCs intensely depends on the temperature.

## 2. Experimentation

The synthesis and characterization of organic dyes has been described in the supplementary information. As purchased $TiO_2$ (T/SP 41112, Solaronix) paste was tape casted on FTO coated conductive glass substrates (7Ω/seq) and then heated at 450 °C for 30 min. Coated films were dipped in the dye solution (2 mM of newly synthesized organic dye in chloroform) for 24 h. The sensitized samples were genteelly washed with ethanol solvent to eradicate the unabsorbed photosensitizer molecules. The platinum paste was tape casted on another FTO glass substrate (Plasticol T), annealed for 20 min at 450 °C. The photoanode and counter electrode were joined together with the help of super glue and electrolyte (Iodolyte Z-50, Solaronix) was inserted between the electrodes.

Visible spectra of photosensitizer in chloroform and adsorbed on $TiO_2$ film were recorded by JASCO-670 spectrophotometer. Current-Voltage characteristics of devices were studied using the IV-5 solar simulator with data acquisition system (PV Measurements Company). A reference silicon solar cell was used to calibrate the system. A potentiostat (Bio-Logic) was used to carry out the EIS analysis of solar devices. The test was performed under 0.7 V forward bias with frequency range of 10 Hz–800 KHz.

## 3. Results and discussion

### 3.1. Electrochemical properties

The energy level orbitals of excited dye must provide necessary thermodynamic driving force for the charge transfer. For effective charge transfer from excited photosensitizer to the conduction band ($E_{CB}$) of semiconductor, the lowest unoccupied molecular orbital (LUMO) of sensitizer must be more negative than the $E_{CB}$ of semiconductor. Similarly, for a fast regeneration of dye, the redox potential of the electrolyte must be more negative than the highest occupied molecular orbital (HOMO) level of photosensitizer [20].

The HOMO, LUMOs and band gap of dye were found out by Density functional theory (DFT) calculations. The simulation was performed on Amsterdam density functional (ADF) program (2013.01). The geometry of photosensitizer was optimized by employing Generalized gradient approximation (GAD) [21] at optimized Lee–Yang–Parr (OLYP) [22], Becke parameter, Lee-Yang-Parr (BLYP) [23], Perdew Wang (PW91) [24,25] and local density approximation (LDA) [26] with triple-ζ polarization (TZP) basis function [27]. The relativistic effects were considered by choosing zero order regular approximation in its scalar approximation [20,28]. All models show approximately the same values of HOMOs, LUMOs and band gaps. Different models were used to justify these values.

Table 1 shows the simulated HOMO, LUMO and band gap of photosensitizer. Fig. 1 shows that the HOMO of the dye with the highest electron density is located at donor group and the LUMO is situated in the anchoring group via π-bridge segment. Consequently, the HOMO-LUMO excitations caused by the incident light could move the electrons from donor to anchoring unit through the π-bridge fragment. These findings advocate that photosensitizer can transfer electrons to the $E_{CB}$ of $TiO_2$.

**Table 1**
FMO and band gaps of dyes sensitizer.

| Models | HOMOs (eV) | LUMOs (eV) | Band Gap (eV) |
|---|---|---|---|
| GAD at BLYP with triple-ζ polarization | −5.15 | −3.90 | 1.25 |
| GAD at OLYP with triple-ζ polarization | −4.86 | −3.69 | 1.18 |
| GAD at PW91 with triple-ζ polarization | −5.30 | −4.04 | 1.26 |
| GAD at PB with triple-ζ polarization | −5.34 | −4.10 | 1.24 |
| LDA with triple-ζ polarization | −5.47 | 4.20 | 1.27 |

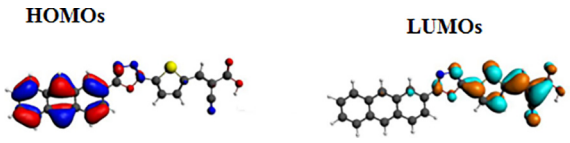


**Fig. 1.** Simulated HOMO and LUMO of the dye.

### 3.2. Optical characteristics of photosensitizer

The absorption spectra of organic dye in chloroform and anchored to $TiO_2$ are shown in Fig. 2. Two different absorption bands of dye in the chloroform can be observed: weak band corresponding to the $\pi$–$\pi^*$ transition of the conjugated molecules is in the range of 380–400 nm and other is about 430–460 nm could be assigned to the intramolecular charge transfer between donor and acceptor anchoring moiety (shown in Fig. 2a). However, the

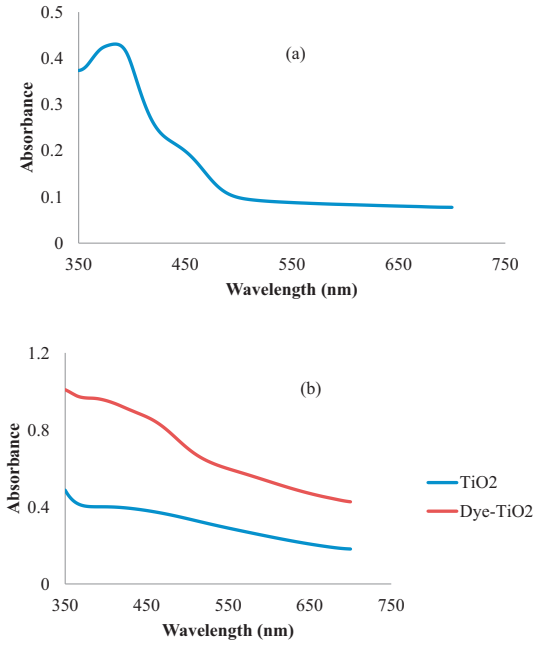


**Fig. 2.** Absorption spectra of (a) dye solution having concentration of 0.1 mM and (b) dye (2 mM solution of dye in chloroform) adsorbed on $TiO_2$.

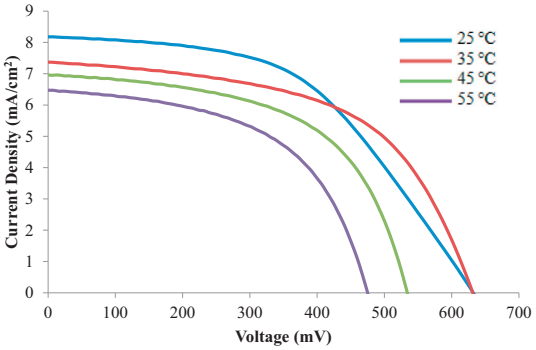


**Fig. 3.** $J_{sc}$-V characteristics of DSSC at different temperatures.

**Table 2**
Photovoltaic properties of DSSCs.

| Temperature (°C) | $J_{sc}$ (mA/cm$^2$) | $V_{oc}$ (mV) | FF (%) | $\eta$ (%) |
|---|---|---|---|---|
| 25 | 8.212 | 632 | 53 | 2.581 |
| 35 | 7.432 | 627 | 55 | 2.567 |
| 45 | 7.003 | 534 | 56 | 2.085 |
| 55 | 6.745 | 475 | 54 | 1.659 |

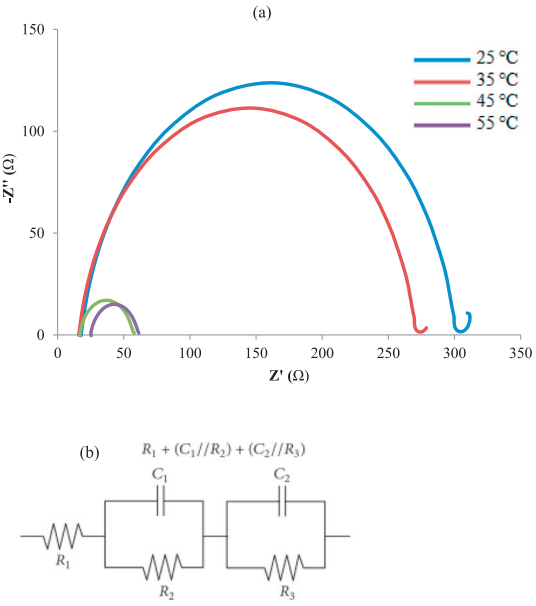


**Fig. 4.** (a) EIS spectra and (b) equivalent circuit of DSSCs.

maximum absorption peak of dye is red shifted when anchored to $TiO_2$ film (shown in Fig. 2b) due to the interaction between the carboxylate group and the surface $Ti^{4+}$ ions. This interaction leads to increase the delocalization of the $\pi^*$ orbital and on the contrary red shift of absorption spectrum.

### 3.3. Photovoltaic performance of devices

*J*-V characteristics of DSSC at various temperatures are shown in Fig. 3. Photovoltaic parameters such as open circuit voltage ($V_{oc}$) fill factor (FF), short circuit current density ($J_{sc}$), and power conversion efficiency ($\eta$) of DSSCs at 25 °C, 35 °C, 45 °C and 55 °C are listed in Table 2. The results indicate that the PCE of DSSC strongly depends on temperature and the cell is stable up to 35 °C. However above 35 °C, the PCE of device exponentially reduces with increasing temperature. This decrease in efficiency is mainly attributed to decrease in voltage with increasing temperature. Open circuit voltage of DSSC is defined as the difference between the quasi-Fermi level of $TiO_2$ photoelectrode and the redox energy level of the electrolyte under illumination. In DSSCs, variation of $V_{oc}$ can be explained by a shift of the potential of the $TiO_2$ conduction band edge. The band gap of semiconductor ($TiO_2$) decreases with temperature [29,30]. Due to this decrease in the band gap of $TiO_2$ more incident energy is absorbed by the $TiO_2$ hence it requires less energy to raise electrons to the conduction band. This results in the large photocurrent through the $TiO_2$, which consequently implies that there is decrease in the voltage. Other photovoltaic parameters like $J_{sc}$ and FF do not remarkably change with temperature. The error bars of photovoltaic parameters of DSSCs at 35 °C show that results are highly reproducible (see the supplementary information: Fig. S5).

**Table 3**
Charge combination resistance at $TiO_2$/dye/electrolyte interface of DSSCs at different temperatures.

| Temperature (°C) | $R_3$ (Ohm) |
|---|---|
| 25 | 282.40 |
| 35 | 251.32 |
| 45 | 40.340 |
| 55 | 35.061 |

### 3.4. EIS measurement

EIS analysis was conducted to analyze the effect of temperature on the interface resistances of DSSCs. The Nyquist plots of DSSCs are shown in Fig. 4a. The junction impedance represented by equivalent circuit diagram is shown in Fig. 4b. The Nyquist plot of DSSCs is normally characterized by three semicircles. The resistance at electrode/electrolyte interface is represented by the first semicircle ($R_2$), and interface resistance photoanode/electrolyte is denoted by second semicircle ($R_3$). While the diffusion of $I^-/I_3^-$ in electrolyte ($Zw$) is epitomized by third semicircle [31,32]. Here in this case we observed only the second arc of $R_3$ in the Nyquist plot (Fig. 4). It means that the other two arcs corresponding to $R_2$ and $Zw$ are overshadowed by this large semicircle of $R_3$ [33,34]. The $R_3$ signifies the charge recombination resistance, e.g., a larger $R_3$ specifies a slower charge recombination. $R_3$ of sensitizer at different temperature is also presented in Table 3. The results signify that the temperature accelerates the charge recombination process. In a DSSC the conduction band shift of the $TiO_2$ film and recombination and charges transport kinetics are influenced by the cell temperature [35,36]. The driving force for recombination is related to the energy level (where the electrons are located), and the temperature, both of which are related to the rate constant, $k_r$(T), and the electron concentration [37]. As $V_{oc}$ changes, the Fermi level (EF) in $TiO_2$ moves towards or away from the conduction band edge ($E_{CB}$). When the Fermi level moves up, the respective electron traps below are filled and in this condition, it can be expected that the activation energy ($E_a$) of recombination is proportional to ($E_{CB} - E_F$) [38].

Moreover, the variation of $V_{oc}$ with temperature can also be explained in terms of electron lifetime [29]. Open circuit voltage decreases with the decrease of electron lifetime owing to an increase of charge recombination. Increase of charge recombination caused by the temperature resulted in decrease in an electron lifetime. As a consequence, a reduction in an open-circuit voltage ($V_{oc}$) was achieved. The decline in photovoltage (due to decrease in charge recombination resistance) with the rise of temperature is in the order of 25 °C ($R_3$ = 282 Ohm and $V_{oc}$ = 632 mV) > 35 °C ($R_3$ = 251 Ohm and $V_{oc}$ = 627 mV) > 45 °C ($R_3$ = 40 Ohm and $V_{oc}$ = 534 mV) > 55 °C ($R_3$ = 35 Ohm and $V_{oc}$ = 475 mV).

## 4. Conclusion

DFT simulation results demonstrate that the LUMO of the dye is larger than the $E_{CB}$ of $TiO_2$. Thus, the injection of electrons from sensitizer to the $E_{CB}$ of $TiO_2$ is thermodynamically possible. Photovoltaic measurements show that the efficiency of DSSC decreases with temperature. The drop in efficiency is mainly attributed to a decrease in photo-voltage with temperature. EIS analysis demonstrates that the charge recombination resistance also decreases with an increase of temperature owing to the decrease of an electron lifetime. The overall results recommend that 1,3,4-oxadiazol based DSSCs with an electrolyte (Iodolyte Z-150, Solaronix) is stable up to 35 °C. Thus, it can be concluded that the liquid electrolyte based DSSCs in the conversion of solar energy to electricity is not favorable for high ambient temperature environment.

## Acknowledgment

The authors acknowledge the support rendered by the CoRE-RE, KFUPM.

## Appendix A. Supplementary data

Supplementary data associated with this article can be found, in the online version, at https://doi.org/10.1016/j.matlet.2018.03.055.

## References

[1] B. O'Regan, M. Grätzel, A low-cost, high-efficiency solar cell based on dye-sensitized colloidal TiO2 films, Nature 353 (1991) 737–740, https://doi.org/10.1038/353737a0.
[2] J.-H. Yum, P. Chen, M. Grätzel, M.K. Nazeeruddin, Recent developments in solid-state dye-sensitized solar cells, ChemSusChem 1 (2008) 699–707, https://doi.org/10.1002/cssc.200800084.
[3] S. Mathew, A. Yella, P. Gao, R. Humphry-Baker, B.F.E. Curchod, N. Ashari-Astani, et al., Dye-sensitized solar cells with 13% efficiency achieved through the molecular engineering of porphyrin sensitizers, Nat. Chem. 6 (2014) 242–247, https://doi.org/10.1038/nchem.1861.
[4] U. Mehmood, K. Harrabi, I.A. Hussein, S. Ahmed, Enhanced photovoltaic performance of dye-sensitized solar cells using $TiO_2$-graphene microplatelets hybrid photoanode, IEEE J. Photovoltaics (2015) 1–6, https://doi.org/10.1109/JPHOTOV.2015.2479468.
[5] M.K. Nazeeruddin, F. De Angelis, S. Fantacci, A. Selloni, G. Viscardi, P. Liska, et al., Combined experimental and DFT-TDDFT computational study of photoelectrochemical cell ruthenium sensitizers, J. Am. Chem. Soc. 127 (2005) 16835–16847, https://doi.org/10.1021/ja052467l.
[6] U. Mehmood, S. Ahmed, I.A. Hussein, K. Harrabi, Improving the efficiency of Dye sensitized solar cells by TiO2–graphene nanocomposite photoanode, Photonics Nanostruct. Fundam. Appl. (2015), https://doi.org/10.1016/j.photonics.2015.08.003.
[7] F. Gao, Y. Wang, D. Shi, J. Zhang, M. Wang, X. Jing, et al., Enhance the optical absorptivity of nanocrystalline TiO2 film with high molar extinction coefficient ruthenium sensitizers for high performance dye-sensitized solar cells, J. Am. Chem. Soc. 130 (2008) 10720–10728, https://doi.org/10.1021/ja801942j.
[8] C.-Y. Chen, M. Wang, J.-Y. Li, N. Pootrakulchote, L. Alibabaei, C.-H. Ngoc-le, et al., Highly efficient light-harvesting ruthenium sensitizer for thin-film dye-sensitized solar cells, ACS Nano 3 (2009) 3103–3109, https://doi.org/10.1021/nn900756s.
[9] Umer Mehmood, Saleem-ur Rahman, Khalil Harrabi, Ibnelwaleed A. Hussein, B. V.S. Reddy, Recent advances in dye sensitized solar cells, Adv. Mater. Sci. Eng. 2014 (2014) 12, https://doi.org/10.1155/2014/974782.
[10] Umer Mehmood, Saleem-ur Rahman, Khalil Harrabi, Ibnelwaleed A. Hussein, B. V.S. Reddy, Recent advances in dye sensitized solar cells, Adv. Mater. Sci. Eng. 2014 (2014) 12, https://doi.org/10.1155/2014/974782.
[11] C. Wang, G.-Y. Jung, Y. Hua, C. Pearson, M.R. Bryce, M.C. Petty, et al., An efficient pyridine- and oxadiazole-containing hole-blocking material for organic light-emitting diodes: synthesis, crystal structure, and device performance, Chem. Mater. 13 (2001) 1167–1173, https://doi.org/10.1021/cm0010250.
[12] D. Joly, L. Pellejà, S. Narbey, F. Oswald, J. Chiron, J.N. Clifford, et al., A robust organic dye for dye sensitized solar cells based on iodine/iodide electrolytes combining high efficiency and outstanding stability, Sci. Rep. 4 (2014) 4033, https://doi.org/10.1038/srep04033.
[13] D. Högberg, B. Soberats, S. Uchida, M. Yoshio, L. Kloo, H. Segawa, et al., Nanostructured two-component liquid-crystalline electrolytes for high-temperature dye-sensitized solar cells, Chem. Mater. 26 (2014) 6496–6502, https://doi.org/10.1021/cm503090z.
[14] H.-S. Lee, S.-H. Bae, Y. Jo, K.-J. Kim, Y. Jun, C.-H. Han, A high temperature stable electrolyte system for dye-sensitized solar cells, Electrochim. Acta 55 (2010) 7159–7165, https://doi.org/10.1016/j.electacta.2010.07.011.
[15] Egbert Figgemeier, Anders Hagfeldt, Are dye-sensitized nano-structured solar cells stable: An overview of device testing and component analyses, Int. J. Photoenergy 6 (2004) 127–140.
[16] M.I. Asghar, K. Miettunen, J. Halme, P. Vahermaa, M. Toivola, K. Aitola, et al., Review of stability for advanced dye solar cells, Energy Environ. Sci. 3 (2010) 418, https://doi.org/10.1039/b922801b.
[17] M. Grätzel, Photovoltaic performance and long-term stability of dye-sensitized meosocopic solar cells, Comptes Rendus Chim 9 (2006) 578–583, https://doi.org/10.1016/j.crci.2005.06.037.
[18] S. Dai, J. Weng, Y. Sui, S. Chen, S. Xiao, Y. Huang, et al., The design and outdoor application of dye-sensitized solar cells, Inorg. Chim. Acta 361 (2008) 786–791, https://doi.org/10.1016/j.ica.2007.04.018.
[19] P. Sommeling, M. Späth, H.J. Smit, N. Bakker, J. Kroon, Long-term stability testing of dye-sensitized solar cells, J. Photochem. Photobiol. A Chem. 164 (2004) 137–144, https://doi.org/10.1016/j.jphotochem.2003.12.017.
[20] U. Mehmood, I.A. Hussein, M. Daud, S. Ahmed, K. Harrabi, Theoretical study of benzene/thiophene based photosensitizers for dye sensitized solar cells (DSSCs), Dye. Pigment 118 (2015) 152–158, https://doi.org/10.1016/j.dyepig.2015.03.003.
[21] J.P. Perdew, K. Burke, M. Ernzerhof, Generalized gradient approximation made simple, Phys. Rev. Lett. 77 (1996) 3865–3868, https://doi.org/10.1103/PhysRevLett. 77.3865.
[22] M. Swart, A.W. Ehlers, K. Lammertsma, Performance of the OPBE exchange-correlation functional, Mol. Phys. 102 (2004) 2467–2474, https://doi.org/10.1080/00268970420002750l7.
[23] J.P. Finley, Using the local density approximation and the LYP, BLYP and B3LYP functionals within reference-state one-particle density-matrix theory, Mol. Phys. 102 (2004) 627–639, https://doi.org/10.1080/00268970410001687452.
[24] J.F. Dobson, G. Vignale, M.P. Das (Eds.), Electronic Density Functional Theory, Springer US, Boston, MA, 1998, https://doi.org/10.1007/978-1-4899-0316-7.
[25] M.D. Patey, C.E.H. Dessent, A PW91 density functional study of conformational choice in 2-phenylethanol, n-butylbenzene, and their cations: problems for density functional theory?, J Phys. Chem. A 106 (2002) 4623–4631, https://doi.org/10.1021/jp012966i.
[26] M.E. Casida, C. Jamorski, K.C. Casida, D.R. Salahub, Molecular excitation energies to high-lying bound states from time-dependent density-functional response theory: Characterization and correction of the time-dependent local density approximation ionization threshold, J. Chem. Phys. 108 (1998) 4439, https://doi.org/10.1063/1.475855.
[27] C.D. Sherrill, M.L. Leininger, T.J. Van Huis, H.F. Schaefer, Structures and vibrational frequencies in the full configuration interaction limit: Predictions for four electronic states of methylene using a triple-zeta plus double polarization (TZ2P) basis, J. Chem. Phys. 108 (1998) 1040, https://doi.org/10.1063/1.475465.
[28] U. Mehmood, I.A. Hussein, K. Harrabi, B.V.S. Reddy, Density functional theory study on dye-sensitized solar cells using oxadiazole-based dyes, J. Photonics Energy 5 (2015) 53097, https://doi.org/10.1117/1.JPE.5.053097.
[29] A. Usami, S. Seki, Y. Mita, H. Kobayashi, H. Miyashiro, N. Terada, Temperature dependence of open-circuit voltage in dye-sensitized solar cells, Sol. Energy Mater. Sol. Cells 93 (2009) 840–842, https://doi.org/10.1016/j.solmat.2008.09.040.
[30] B.C. O'Regan, J.R. Durrant, Calculation of activation energies for transport and recombination in mesoporous $TiO_2$/dye/electrolyte films–taking into account surface charge shifts with temperature, J. Phys. Chem. B 110 (2006) 8544–8547, https://doi.org/10.1021/jp060979w.
[31] K. Lee, C. Hu, H. Chen, K. Ho, Incorporating carbon nanotube in a low-temperature fabrication process for dye-sensitized $TiO_2$ solar cells, Sol. Energy Mater. Sol. Cells 92 (2008) 1628–1633, https://doi.org/10.1016/j.solmat.2008.07.012.
[32] Y.-L. Xie, Z.-X. Li, Z.-G. Xu, H.-L. Zhang, Preparation of coaxial $TiO_2$/ZnO nanotube arrays for high-efficiency photo-energy conversion applications, Electrochem. Commun. 13 (2011) 788–791, https://doi.org/10.1016/j.elecom.2011.05.003.
[33] S. Li, Y. Lin, W. Tan, J. Zhang, X. Zhou, J. Chen, et al., Preparation and performance of dye-sensitized solar cells based on ZnO-modified $TiO_2$ electrodes, Int. J. Miner. Metall. Mater. 17 (2010) 92–97, https://doi.org/10.1007/s12613-010-0116-z.
[34] A.S. Nair, R. Jose, Y. Shengyuan, S. Ramakrishna, A simple recipe for an efficient $TiO_2$ nanofiber-based dye-sensitized solar cell, J. Colloid Interface Sci. 353 (2011) 39–45, https://doi.org/10.1016/j.jcis.2010.09.042.
[35] M. Wang, P. Chen, R. Humphry-Baker, S.M. Zakeeruddin, M. Grätzel, The influence of charge transport and recombination on the performance of dye-sensitized solar cells, Chemphyschem 10 (2009) 290–299, https://doi.org/10.1002/cphc.200800708.
[36] A. Kongkanand, P.V. Kamat, Electron storage in single wall carbon nanotubes. Fermi level equilibration in semiconductor-SWCNT suspensions, ACS Nano 1 (2007) 13–21, https://doi.org/10.1021/nn700036f.
[37] B. O'Regan, L. Xiaoe, T. Ghaddar, Dye adsorption, desorption, and distribution in mesoporous $TiO_2$ films, and its effects on recombination losses in dye sensitized solar cells, Energy Environ. Sci. 5 (2012) 7203, https://doi.org/10.1039/c2ee21341a.
[38] J. Maçaira, I. Mesquita, L. Andrade, A. Mendes, Role of temperature in the recombination reaction on dye-sensitized solar cells, Phys. Chem. Chem. Phys. 17 (2015) 22699–22710, https://doi.org/10.1039/c5cp02942b.